Dynamics of a paired optical vortex generated by second-harmonic generation

Y. Toda, S. Honda, R. Morita

Department of Applied Physics, Hokkaido University, N13W8 Kita-ku, Sapporo, Japan

toda@eng.hokudai.ac.jp

Abstract: We study the dynamics of a paired optical vortex (OV) generated by second-harmonic generation (SHG) using sub-picosecond pulses. By changing the position of a thin nonlinear crystal along the propagation direction, we observe a rotation of two vortices with changing separation distance. The dynamics is well explained by SHG with a beam walk-off, which introduces a contamination of zero-order Laguerre-Gaussian beam (LG_0) together with topological charge doubling. The quantitative analysis indicates that the rotation angle of the OVs manifests the Gouy phase while the splitting provides the walk-off angle of the crystal. We also show that the subtraction of LG_0 is realized by the superposition of LG_0 with an anti-balanced phase in the pump.

OCIS codes: (050.4865) Optical vortices; (190.2620) Frequency conversion; (190.0190), Nonlinear optics; (260.6042) Singular Optics.

References and links

1. K. T. Gahagan and G. A. Swartzlander, Jr., "Optical vortex trapping of particles," Opt. Lett. **21**, 827–829 (1996).
2. D. G. Grier, "A revolution in optical manipulation," Nature **424**, 810–816 (2003).
3. Y. Tokizane, K. Shimatake, Y. Toda, K. Oka, M. Tsubota, S. Tanda, and R. Morita, "Global evaluation of closed-loop electron dynamics in quasi-one-dimensional conductors using polarization vortices," Opt. Express **17**, 24198–24207 (2009).
4. G. Gibson, J. Courtial, M. J. Padgett, M. Vasnetsov, V. Pas'ko, S. M. Barnett, and S. Franke-Arnold, "Free-space information transfer using light beams carrying orbital angular momentum," Opt. Express **12**, 5448–5456 (2004).
5. L. Allen, M. W. Beijersbergen, R. J. C. Spreeuw, and J. P. Woerdman, "Orbital angular momentum of light and the transformation of Laguerre-Gaussian laser modes," Phys. Rev. A **45,** 8185–8189 (1992).
6. M. Berry, "Making waves in physics," Nature **403**, 21–21 (2000).
7. M.J. Paz-Alonso and H. Michinel, "Superfluidlike Motion of Vortices in Light Condensates," Phys. Rev. Lett. **94** 093901-1–4 (2005).
8. I. V. Basistiy, V. Y. Bazhenov, M. S. Soskin, and M. V. Vasnetsov, "Optics of light-beams with screw dislocations," Opt. Commun. **103**, 422–428 (1993).
9. K. Staliunas, "Dynamics of optical vortices in a laser beam," Opt. Commun. **90**, 123–127 (1992).
10. G. Indebetow, "Optical vortices and their propagation," J. Mod. Opt. **40**, 73–87 (1993).
11. M. S. Soskin, V. N. Gorshkov, M. V. Vasnetsov, J. T. Malos, and N. R. Heckenberg, "Topological charge and angular momentum of light beams carrying optical vortices," Phys. Rev. A **56**, 4064–4075 (1997).
12. D. Rozas, C. T. Law, G. A. Swartzlander, "Propagation dynamics of optical vortices," J. Opt. Soc. Am. B **14**, 3054–3065 (1997).
13. I. Freund, "Optical vortex trajectories," Opt. Commun. 181, 19–33 (2000). I. D. Maleev, and G. A. Swartzlander, "Composite optical vortices," J. Opt. Soc. Am. B **20**, 1169–1176 (2003).
14. K. Dholakia, N. B. Simpson, M. J. Padgett, and L. Allen, "Second-harmonic generation and the orbital angular momentum of light," Phys. Rev. A **54**, R3742–3745 (1996).
15. A. Beržanskis, A. Matijošius, A. Piskarskas, V. Smilgevičius, and A. Stabinis, "Sum-frequency mixing of optical vortices in nonlinear crystals," Opt. Commun. **150**, 372–280 (1998).

#130018 - $15.00 USD Received 15 Jun 2010; revised 21 Jul 2010; accepted 28 Jul 2010; published 3 Aug 2010

16. F. Flossmann, U. T. Schwarz, M. Maier, and M. R. Dennis, "Polarization singularities from unfolding an optical vortex through a birefringent crystal," Phys. Rev. Lett. **95**, 253901-1–4 (2005).
17. A. Dreischuh, D. N. Neshev, V. Z. Kolev, S. Saltiel, M. Samoc, W. Krolikowski, and Y. S. Kivshar, "Nonlinear dynamics of two-color optical vortices in lithium niobate crystals," Opt. Express **16**, 5406–5420 (2008).
18. M. W. Beijersbergen, L. Allen, H. Van der Veen, and J. P. Woerdman, "Astigmatic laser mode converters and transfer of orbital angular momentum," Opt. Commun. **96**, 123–132 (1993).
19. Y. Yoshikawa, H. Sasada, "Versatile generation of optical vortices based on paraxial mode expansion," J. Opt. Soc. Am. A **19**, 2127–2133 (2002).
20. K. Kato, "Second-harmonic generation to 2048 Åin β-BaB_2O_4," IEEE J. Quantum Electron., **QE-22**, 1013–1014 (1986).
21. S. M. Baumann, D. M. Kalb, L. H. MacMillan, E. J. Galvez, "Propagation dynamics of optical vortices due to Gouy phase," Opt. Express **17**, 9818–9827 (2009).
22. J. H. Chow, G. de Vine, M. B. Gray, and D. E. McClelland, "Measurement of Gouy phase evolution by use of spatial mode interference," Opt. Lett. **29**, 2339–2341 (2004).
23. J. Hamazaki, Y. Mineta, K. Oka, and R. Morita, gDirect observation of Gouy phase shift in a propagating optical vortex," Opt. Express **14**, 8382–8392 (2006).
24. A. Bahabad and A. Arie, "Generation of optical vortex beams by nonlinear wave mixing," Opt. Express **15**, 17619–17624 (2007).
25. Y. Ueno, Y. Toda, S. Adachi, R. Morita and T. Tawara, "Coherent transfer of orbital angular momentum to excitons by optical four-wave mixing," Opt. Express **17**, 20567–20574 (2009).

1. Introduction

Optical vortices (OVs) have been studied extensively in recent years owing to their various potential applications, such as laser trapping [1], spatially-resolved imaging [2], spectroscopy [3] and information processing [4]. The OVs are associated with a series of Laguerre-Gaussian (LG) modes LG_ℓ^p of the paraxial wave equation, where ℓ and p are integer. The index ℓ is so-called topological charge or orbital angular momentum (OAM), given by the winding number of phase on the wavefront around the vortex [5]. The phase singularity also characterizes a null intensity of the beam cross section. Another parameter p denotes the number of nodal rings about the beam axis. In the paper, we will focus our attention on singly-ringed LG_ℓ^0 modes, and hereafter describe as LG_ℓ. Since vortices make an important role in various branches of physics, such as fluid mechanics, condensed matter physics, and astrophysics, the study of OVs provides a universal viewpoint in optical physics and thus has attracted fundamental interest as well [6, 7].

Of the various fundamental studies, the propagation/interaction dynamics induced by the superposition of the OVs with different charges (composite OVs) have been intensively investigated. In general, the superposition of coherent light fields produces a phase distribution different from that of the component fields. In the case of OVs, owing to the topological phase singularities, composite vortices show characteristic changes along with propagation, such as creation and annihilation of a vortex, attraction, repulsion and rotation of vortex pairs. Since around 1990, numerous theoretical/experimental studies have established a comprehensive framework for analyzing the composite OVs [8, 9, 10, 11, 12, 13]. One of the experimental foundations was laid in [8], where the authors showed that the splitting of a vortex with a charge $\ell(|\ell| > 1)$ into $|\ell|$ vortices with a single charge is a common property and that it is reversible by superposition with a Hermite-Gaussian ($HG_{00} \equiv LG_0$) beam. They also demonstrated the second-harmonic generation (SHG) with a paired single-charge OV ($\ell = 1 + 1$) from the OV beam with $\ell = 1$, suggesting the SHG formed by LG_0+LG_2. In principle, the OAM is transformed by SHG (in the particular case of [14] from a $\ell = 1$ beam to a $\ell = 2$ beam). Therefore the perturbation of LG_0 can be attributed to the breakdown of the OAM symmetry (azimuthal symmetry) associated with the SHG process, such as beam walk-off (birefringence) in nonlinear crystals [15, 16].

In this paper, we investigate an interaction of a paired OV generated by SHG in a thin BBO (β-Barium Borate) crystal. By changing the crystal position along the propagation direction,

#130018 - $15.00 USD Received 15 Jun 2010; revised 21 Jul 2010; accepted 28 Jul 2010; published 3 Aug 2010

a rotational dynamics of the paired OV including creation and collapse of pairing is observed and quantitatively analyzed. Each dynamics observed in the experiment is well reproduced by the theoretical simulation based on the beam walk-off, which produces the changes in relative amplitude and phase of the composite OVs (LG_0+LG_2) according to the position of the nonlinear crystal. The experiment is simple but provides an accurate evolution of the vortices without changing neither the propagation distance nor crystal length. We also demonstrate the compensation of the walk-off effect by superimposing the LG_0 beam in the pump.

2. Second-harmonic vortices with a beam walk-off

In nonlinear wave-conversion/mixing, the crystal asymmetry easily breaks the azimuthal symmetry for OAM conversion. One of the major contributions is given by the walk-off of the nonlinear crystal [15, 16]. The pump depletion (back conversion from the second-harmonic beam to the fundamental beam) also plays an important role in the SHG pumped by a vortex beam [17]. We neglect this process assuming the SHG with low conversion efficiency. In the experimental section, we will show the dynamics of a paired OV as a function of the crystal position. The purpose of this section is to see how the beam walk-off affects the relative amplitude and phase of the second-harmonic OVs according to the crystal position.

In the paper, we restrict our consideration to the case of type I phase-matching between the ordinary fundamental ($o+o$) and extraordinary second-harmonic(e) beams . We also assume the crystal thickness is thin enough to satisfy the weak walk-off regime. The comprehensive analysis for various phase-matching conditions can be found elsewhere [15].

We first introduce the basic equations of the propagating OV (corresponds to the fundamental beam in the SHG process). The polarization of the beam is linear and coincides with a principle axis of the uniaxial crystal. Within the framework of paraxial wave equation, the complex electric field of the continuous OV with a topological charge ℓ, frequency ω and wavenumber k is given by

$$E(r,\varphi,z,t) = E_0 u_\ell(r,\varphi,z)\exp\left[i(kz-\omega t)\right], \tag{1}$$

where r, φ, and z are the cylindrical coordinates, and E_0 is the amplitude parameter. u_ℓ is the envelope function of the LG_ℓ mode denoted as [5, 11]

$$u_\ell(r,\varphi,z) = a_\ell(r,\varphi,z)e^{-i\Phi_G^\ell(z)} = \frac{w_0}{w(z)}\left(\frac{r}{w(z)}\right)^{|\ell|} e^{i\ell\varphi}e^{-r^2/w(z)^2}e^{-i\Phi_G^\ell(z)}. \tag{2}$$

Here we neglect the wavefront curvature. The Gouy phase Φ_G^ℓ and beam size $w(z)$ are given by

$$\Phi_G^\ell(z) = (|\ell|+1)\tan^{-1}(z/z_R), \;\; w(z) = w_0\sqrt{1+(z/z_R)^2}, \tag{3}$$

with the beam waist w_0 and Rayleigh range $z_R = kw_0^2/2$.

We start considering the SHG process with a walk-off [15]. Since the walk-off breaks the azimuthal symmetry, we rewrite the factor a_ℓ in Cartesian coordinates as

$$a_\ell(x,y,z) = \frac{w_0}{w(z)}\left(\frac{x\pm iy}{w(z)}\right)^{|\ell|} e^{-\left(x^2+y^2\right)/w(z)^2}, \tag{4}$$

where $x+iy$ ($x-iy$) is taken for positive (negative) ℓ. From the coupled wave equations in a quadratic nonlinear crystal, the ordinary polarized fundamental and extraordinary second-harmonic field amplitudes (E^F and E^S) follow the equations

$$\frac{\partial E^S}{\partial z} = -\alpha\frac{\partial E^S}{\partial x} + gE^F E^F, \qquad \frac{\partial E^F}{\partial z} = 0, \tag{5}$$

#130018 - $15.00 USD Received 15 Jun 2010; revised 21 Jul 2010; accepted 28 Jul 2010; published 3 Aug 2010

where α is the walk-off angle of the extraordinary second-harmonic beam, and g is the coupling coefficients. We note again that the pump depletion is neglected owing to the low conversion efficiency. Since we consider a thin crystal (thickness L), the beam size can be fixed to be constant throughout the crystal. At the center position of the crystal z', the coupled amplitude equation becomes

$$\frac{\partial E^S}{\partial z} = -\alpha \frac{\partial E^S}{\partial x} + gE^F(x,y,z')E^F(x,y,z'). \tag{6}$$

We note that the envelope function of E^F is given by Eq. (4). For $x_1 = x - \alpha z$, we obtain

$$E^S(x_1,y,z') = g\int_0^L E^F(x_1,y,z')E^F(x_1,y,z')dz. \tag{7}$$

To simplify the equation, we choose the normalization of the coordinates, $\xi = x/w(z')$, $\eta = y/w(z')$, $t = z/L$ and assume $\gamma = \alpha L/w(z')$, $F = (w_0/w(z'))^2 E^S/(gL)$. The second-harmonic envelope at the crystal position z' in Eq. (7) can be transformed to

$$F(\xi,\eta) = e^{-2\eta^2}\int_0^1 (\xi - \gamma t + i\eta)^{2|\ell|} e^{-2(\xi-\gamma t)^2} dt. \tag{8}$$

We now consider the simple case of the fundamental beams with $\ell = 1$. Taking into account the assumption that the crystal is sufficiently thin, Eq. (8) gives

$$\begin{aligned} F(\xi,\eta) &= e^{-2\eta^2}\int_0^1 (\xi - \gamma t + i\eta)^2 e^{-2(\xi-\gamma t)^2} dt \\ &\approx \left[\xi - \frac{\gamma}{2} + i\left(\eta - \frac{\gamma}{2\sqrt{3}}\right)\right]\left[\xi - \frac{\gamma}{2} + i\left(\eta + \frac{\gamma}{2\sqrt{3}}\right)\right]. \end{aligned} \tag{9}$$

The latter approximation holds for $|\xi|, |\eta| \ll 1$, which is consistent with the weak walk-off condition. $F(\xi,\eta) = 0$ results in two vortices at $(\xi_0,\eta_0) = (\gamma/2, \pm\gamma/(2\sqrt{3}))$. Here, it should be noted that, while the usual walk-off between fundamental and second-harmonic waves occur in x-direction, another type of walk-off, that is, singular-point splitting arises in y-direction. In this case, the envelope function of SHG amplitude can be described by a product of two vortices,

$$u_2^S(x,y,z') = ga_1(x - s_1, y - s_2, z')a_1(x - s_1, y + s_2, z')e^{-i2\Phi_G^1(z')}, \tag{10}$$

where $s_1 = \alpha L/2$ and $s_2 = \alpha L/(2\sqrt{3})$. The splitting of the vortices occurs in the y-direction (crystal axis) with a separation of $2s_2 = \alpha L/\sqrt{3}$. Equation (10) follows

$$\begin{aligned} u_2^S(x,y,z') &= ge^{-2s_2^2/w(z')^2}\left(\frac{w_0}{w(z')}\right)^2 \frac{(x - s_1 + iy)^2 + s_2^2}{w(z')^2} e^{-\left\{2(x-s_1)^2 + 2y^2\right\}/w(z')^2} e^{-i2\Phi_G^1(z')} \\ &= ge^{-2s_2^2/w(z')^2} e^{-i(\Phi_G^0(z') + \Phi_G^2(z'))}\left[u_2(x - s_1, y, z')e^{i\Phi_G^2(z')} + \left(\frac{s_2}{w(z')}\right)^2 u_0(x - s_1, y, z')e^{i\Phi_G^0(z')}\right], \end{aligned} \tag{11}$$

showing a superposition of LG_0 and LG_2 with different amplitude and phase. The amplitude of the second-harmonic beam consisting of a product of two vortices thus can be transformed to a series of OVs with different charges. It should be emphasized here that a simple SHG process with a walk-off introduces a contamination of $\ell = 0$ beam together with topological charge doubling. In addition, both the relative amplitude $\propto 1/w^2$ and phase difference $\Phi_G^2 - \Phi_G^0$ depends on z'. As a result, we can evaluate the interaction dynamics of the paired vortex as a function of the crystal position in z-direction.

#130018 - $15.00 USD Received 15 Jun 2010; revised 21 Jul 2010; accepted 28 Jul 2010; published 3 Aug 2010

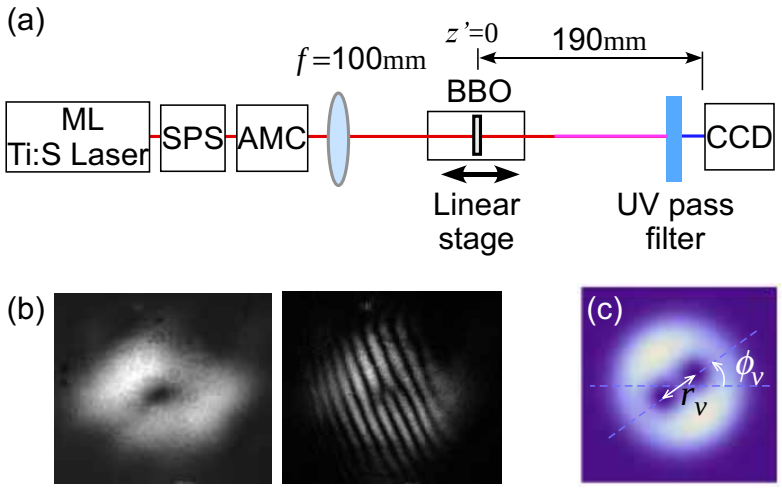

Fig. 1. (a) Schematic illustration of SHG setup. The HG_{00} (TEM_{00}) beam from 100 femtosecond (fs) mode-locked Ti:sapphire (ML: TiS) is converted to a doughnut-like LG_1 by using a spatial phase shifter (SPS) and an astigmatic mode converter (AMC). The second-harmonic OVs are generated by focusing onto a thin BBO ($\varnothing$ 5 mm $\times$ 0.1 mm) crystal on a motorized linear stage using a conventional lens (f = 100 mm), and detected by a charge-coupled device (CCD) after passing through a UV-pass filter. The development of the second-harmonic vortices is observed by changing the crystal position along the propagation direction. (b) Observed intensity distribution of fundamental LG_1 (left) and its interferogram with HG_{00} (right). (c) Schematic illustration of the second-harmonic OVs with a charge splitting. The distance (r_v) and rotation angle (ϕ_v) between two vortices are denoted.

3. Experimental

We investigate the interaction dynamics of the second-harmonic OVs generated by LG_1 pump. Figure 1 (a) shows the schematic of the experimental setup. A mode-locked Ti:sapphire laser with a repetition rate of $\sim$90 MHz and a center wavelength of $\sim$800 nm was used for the light source. The LG_1 pulse (fundamental pulse for the SHG) was created from the HG_{00} pulse from the laser by passing through a spatial phase shifter (SPS) and an astigmatic mode converter (AMC) [18]. The SPS consists of two thin glass plates and inserted into the beam to create a HG_{10} with a relative phase shift of π between the left and right halves of the HG_{00} beam [19]. The HG_{10} pulse is then fed to an astigmatic lens system consisting of two spherical and cylindrical lens.

Figure 1 (b) shows the CCD images of the output of AMC (left), which produces a dark-hole at the center of the beam. To check the topological charge of the pulsed beam, we also demonstrate the interferogram (right in Fig. 1 (b)) with a tilted reference HG_{00} pulse without delay. The fork-like fringe pattern clearly indicates the LG with a topological charge of unity (LG_1) is dominant at this stage. The temporal chirp of the pulse was compensated by a pair of chirp mirrors just after the laser source. The average power of the LG_1 was $\sim$10 mW and its pulse duration evaluated by autocorrelation measurements was $\sim$100 fs.

The LG_1 was focused onto a BBO crystal (CASIX, thickness 0.1 mm) using a lens (f= 100 mm), and the output SHG with type I phase matching was detected by a charge-coupled device (CCD) camera after passing through a UV pass filter. The BBO has a large walk-off angle ($\sim 3.9^\circ$ at 800 nm pump) [20], introducing an azimuthal asymmetry of the second-harmonic

#130018 - $15.00 USD Received 15 Jun 2010; revised 21 Jul 2010; accepted 28 Jul 2010; published 3 Aug 2010

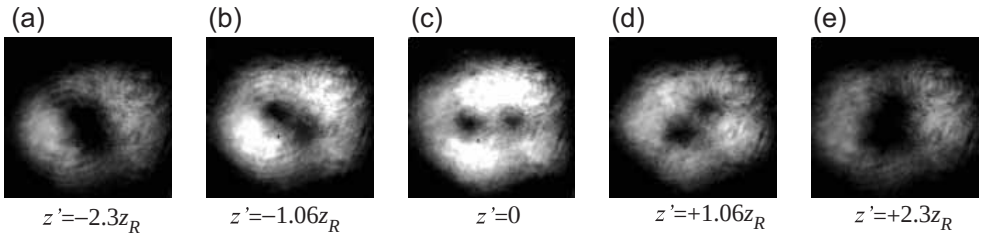

Fig. 2. Observed intensity distributions of a paired second-harmonic vortex at various positions of the BBO crystal (z').

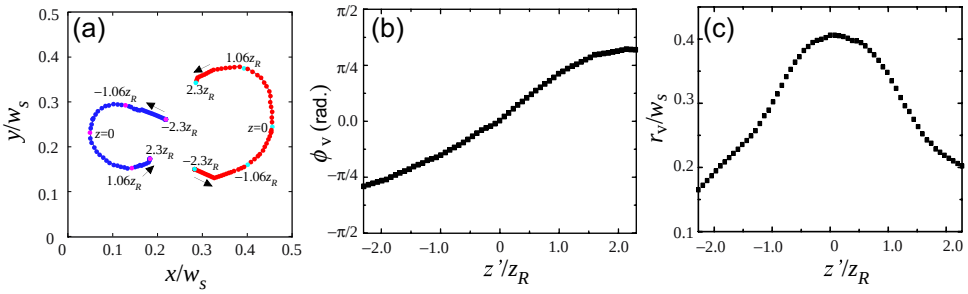

Fig. 3. (a) Trajectories of the second-harmonic vortices at various z'. Plots of different colors show typical positions. Evolutions of (b) ϕ_v and (c) r_v as a function of z'/z_R.

OV even in the thin crystal. The position of the crystal (z') was automatically moved along the optical axis by using a motorized linear stage. The optimum focus position of the input pulse is defined as $z' = 0$, and we obtained the intensity distributions of the SHG over a range between $z' = \pm 7.5$ mm, which corresponds to $z' = \pm 2.3 z_R$ using a Rayleigh length of $z_R (= \pi w_0^2/\lambda \approx 3.3$ mm, where w_0 =29 μm at λ =800 nm). Note that z_R for the fundamental and second-harmonic beams are equal since w_0 of SHG is reduced by a factor of $1/\sqrt{2}$.

Figure 2 shows typical intensity distributions (CCD images) of the SHG at various z'. In Fig. 2 (c), there are two distinct vortices, each of which rotates as a pair together with decreasing the separation as the crystal moves away from $z' = 0$ (Fig. 2 (b) and (d)), and becomes indistinguishable at $|z'| > 2z_R$ (Fig. 2 (a) and (e)). These sequential dynamics can be evaluated as trajectories of the vortices in Fig. 3 (a). Note that we detect the SHG at a fixed position, allowing to evaluate the sequential vortices with the same dimension. For simplicity, we plot the positions of the vortices normalized by the beam size of the SHG (w_s). Following the same manner as the previous reports on the propagation dynamics [12, 21], we also plot the relative angle ϕ_v and distance r_v between the two vortices as a function of the crystal position z'/z_R in Fig. 3 (b) and (c). Here ϕ_v and r_v are denoted in Fig. 1 (c), and reflect the relative phase and amplitude of the composite OVs. As shown in Fig. 3 (b), ϕ_v changes monotonically between $-\pi/2$ and $+\pi/2$, suggesting the Gouy phase rotation [21, 22, 23]. On the other hand, the splitting r_v decreases symmetrically with respect to $z' = 0$, indicating that the perturbation of LG_0 is efficient at $z' = 0$ and decreases as increasing $|z'|$. These z'-dependent splitting suggests the walk-off origin, which will be confirmed below.

We now compare the experimental data with the predictions in Sect.2. The intensity of the vortex field is $I = |u_2^S|^2$ where u_2^S is given by in Eq. (11). In the calculations, only s_2 is a variable parameter to be optimized. We used s_2 =4.1 μm, the validity of which will be discussed later. The intensity distributions of the composite OVs are shown in the upper part of Fig. 4, each

#130018 - $15.00 USD Received 15 Jun 2010; revised 21 Jul 2010; accepted 28 Jul 2010; published 3 Aug 2010

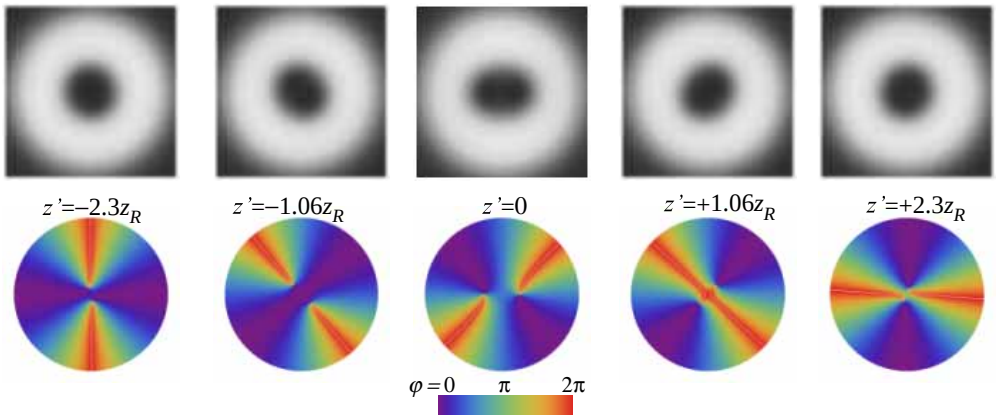

Fig. 4. Calculated intensity (upper) and phase (lower) distributions of the paired second-harmonic vortex at various z'.

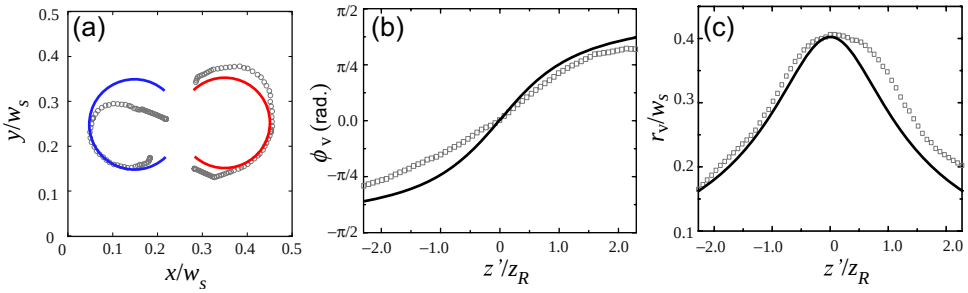

Fig. 5. (a) Calculated trajectories of the second-harmonic vortices at various z'. Evolutions of (b) ϕ_v and (c) r_v as a function of z'/z_R. Experimental plots of Fig. 3 are also shown by gray color.

of which reproduces well the paired OV dynamics in Fig. 2. In the lower part, we also plot the phase distributions in order to clarify the positions of the vortices. Within the focal region, a distinct paired vortex exists owing to the intentional contamination of $\mathrm{LG}_0 \propto 1/w^2$. When moving out of focal region, the pair rotates according to the relative Gouy rotation $\Delta\Phi_G = \Phi_G^2 - \Phi_G^0$, and its separation decreases as LG_0 decreases.

The quantitative comparisons can be realized in Fig. 5, where we re-plot the experimental data of Fig. 3. In Fig. 5 (b), the rotation angle ϕ_v, which reflects the relative phase described by $\Delta\Phi_G = 2\tan^{-1}(z/z_R)$, is consistent with the experimental data. Our simple experiment thus provides an evaluation of the the Gouy phase with a fixed detection geometry. On the other hand, the splitting r_v in Fig. 5 (c) also shows good agreement with experimental results. We note that r_v is determined by the ratio of the amplitude between LG_0 and LG_2, which is given by $(s_2/w)^2$ in Eq. (11). From the experimental data r_v at $z' = 0$, $s_2 (= r_v/2)$ is evaluated to be 4.1 μm. Within the assumption that the beam walk-off is weak, s_2 can be described by $\alpha' L/(2\sqrt{3})$, where α' is the external walk-off angle in the air which satisfies $\sin(\alpha'/\sqrt{3}) = n_e(400\,\mathrm{nm})\sin(\alpha/\sqrt{3})$ from the Snell's law. In the present case, we obtained the internal walk-off angle $\alpha = 5.1^\circ$, which is almost consistent with the typical value of BBO for the type-I phase-matching ($\sim 3.9^\circ$ at 800 nm pump) [20].

The analysis mentioned above successfully demonstrates that the charge splitting due to beam walk-off can be expanded into the composite OVs including LG_0. Therefore we can

#130018 - $15.00 USD Received 15 Jun 2010; revised 21 Jul 2010; accepted 28 Jul 2010; published 3 Aug 2010

remove the splitting by introducing LG_0 (HG_{00}) as another fundamental source. Although such cancellation of LG_0 perturbation using coherent beam addition has already been reported in [8], we employ this technique to compensate the incomplete OAM transfer in the nonlinear conversion process. Since the imperfect OAM restricts the feasibility of OVs, the compensation demonstrated here will contribute to the practical use of the nonlinear OV applications [24, 25].

To prepare such composite OVs ($LG_1+e^{i\varphi_p}LG_0$) in the pump, the laser pulses (HG_{00}) were splitted into two optical paths, one of which transfers HG_{00} to LG_1 using SPS and AMC. Another path carries LG_0 beam through the optical delay line, which consists of a retro-reflector mounted upon a translation stage and a mirror upon a piezoelectric transducer. The former accounts for the difference between two optical paths lengths within the pulse duration while the latter provides a fine position to determine the relative phase φ_p with respect to LG_1. The relative amplitude between LG_1 and LG_0 was controlled by a neutral density filter. The second-harmonic conversion and its detection schemes are the same as in Fig. 1 (a).

The upper part of Fig. 6 shows a series of CCD images of the SHG obtained at various φ_p at a fixed crystal position $z' = 0$. The OV pair changes its separation according to φ_p. A significant

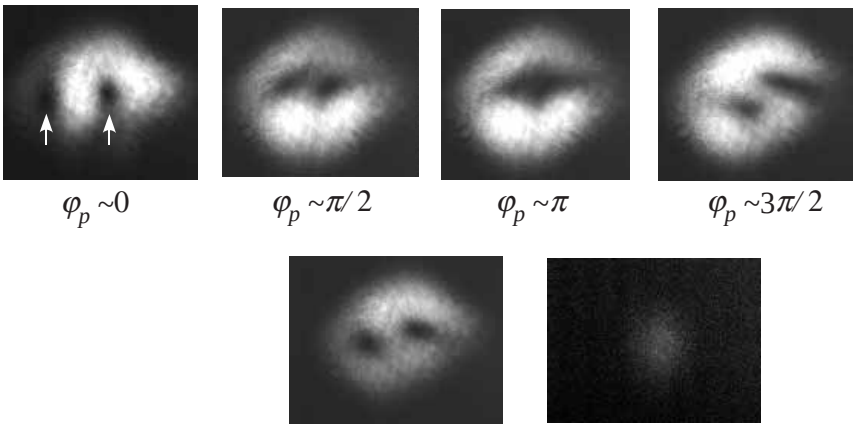

Fig. 6. Intensity distributions of a paired second-harmonic vortex obtained by introducing $LG_1+e^{i\varphi_p}LG_0$. The arrows indicate the vortices for clarity. The crystal is fixed at $z' = 0$. The splitting is reduced significantly by using LG_0 pump pulses with an anti-balanced phase $\varphi_p \sim \pi$. Intensity distributions of SHG obtained by the individual pump pulses (left:LG_1, right:LG_0) are also shown in the lower part.

reduction of the splitting was observed in the anti-phase condition $\varphi_p \sim \pi$. For clarity, the SHG images obtained by introducing individual pump beams (LG_1 and HG_{00}) are shown in the lower part. It is important to note that optimization of the relative amplitude is necessary to realize the absence of splitting. In addition, the optimized amplitude varies with z', indicating that the splitting observed in our experiment does not arise from the fundamental beam but from the SHG.

4. Summary

In summary, we demonstrated an interaction of a paired second-harmonic OV by changing the position of a thin nonlinear crystal (BBO) along the propagation direction. The observed rotational dynamics including creation and collapse of pairing were well reproduced by the theoretical prediction based on the beam walk-off in the crystal. The quantitative analysis indicated that the rotation angle of the paired vortex manifests the Gouy phase while the splitting

#130018 - $15.00 USD Received 15 Jun 2010; revised 21 Jul 2010; accepted 28 Jul 2010; published 3 Aug 2010

provides the walk-off angle of the crystal. The analysis also mentioned that the charge splitting can be expanded into the composite OVs including LG_0, the subtraction of which was experimentally realized by the superposition of LG_0 with an anti-balanced phase in the fundamental beam.

Acknowledgments
This work was supported by Casio foundation, KDDI foundation, and Grant-in-Aid for Scientific Research (B), 2008-2010, No.20360025 from Japan Society for the Promotion of Science (JSPS).

#130018 - $15.00 USD Received 15 Jun 2010; revised 21 Jul 2010; accepted 28 Jul 2010; published 3 Aug 2010